Journal of Great Lakes Research xxx (xxxx) xxx

Contents lists available at ScienceDirect

Journal of Great Lakes Research

journal homepage: www.elsevier.com/locate/jglr

Sediment transport and budget influenced by harbor jetties in storm events

Longhuan Zhu [a,1,*], Guy A. Meadows [a,1], Miraj B. Kayastha [b], Pengfei Xue [a,b,c,1,*]

[a] Great Lakes Research Center, Michigan Technological University, Houghton, MI 49931, United States
[b] Department of Civil, Environmental and Geospatial Engineering, Michigan Technological University, Houghton, MI 49931, United States
[c] Environmental Science Division, Argonne National Laboratory, Lemont, IL 60439, United States

ARTICLE INFO

Communicated by Chin H. Wu

Keywords:
Sediment transport
Sediment budget
Hydrodynamic model
Jetty
Lake Michigan
Great Lakes

ABSTRACT

Accelerated coastal erosion in Lake Michigan has been reported throughout the basin and on regional scales. A significant portion of regional coastal erosion is influenced by coastal structures such as harbor jetties of varying sizes. To understand the effects of coastal structures on local sediment transport and budget, this study focuses on medium-sized harbor jetties at South Haven, MI, in southeastern Lake Michigan, representative of many recreational harbors and harbors of refuge along Great Lakes shorelines. The wave-current-sediment transport processes were simulated using a coupled model, which integrates Simulating Waves Nearshore (SWAN), Finite-Volume Community Ocean Model (FVCOM), and Community Sediment Transport Modeling System (CSTMS). Our results indicate that during storm events, the presence of a pair of jetties consistently leads to a substantial decrease in longshore sediment transport on the downdrift side within a 2 km region. For the entire navigation season from April to December, the storm-time averaged currents and longshore sediment transport are predominantly southward. The jetties increase net sediment transport updrift of the jetties and enhance offshore sediment transport. Simultaneously, they significantly reduce downdrift sediment transport, with persistent eddy structures near the jetty limiting the sediment transported out of the immediate region adjacent to the southern jetty. Consequently, sediment can accrete on both sides of the jetties, potentially widening the beaches. Meanwhile, the region further south of the jetties experiences severe erosion due to a reduced sediment supply from upstream. Understanding the dynamics of sediment transport and budget, particularly with the jetties' influences, is crucial for coastal management.

1. Introduction

Coastal erosion in the Great Lakes has long been driven by an imbalance in the sediment budget, a result of both human activities and natural processes such as wave-current actions associated with water level fluctuations (Leatherman et al., 2000; van Rijn, 2011; Williams et al., 2018). Historical studies consistently document its persistence and impact in the Great Lakes (Barnes et al., 1994; Dilley and Rasid, 1990; Lin and Wu, 2014; Theuerkauf et al., 2019; Troy et al., 2021; Volpano et al., 2020). The erosion significantly damages land, properties, and infrastructure (Meadows et al., 1997; Troy et al., 2021), and also leads to substantial habitat loss and ecosystem disruption (Paprotny et al., 2021; Roebeling et al., 2013; Theuerkauf and Braun, 2021).

Over the past decade, the water level of Lake Michigan, the third largest of the Great Lakes by surface area, has risen rapidly by nearly 2 m from a record-low of 175.57 m (IGLD datum) in January 2013 to a record-high of 177.46 m in July 2020, remaining above the historical average of 176.45 m (https://lre-wm.usace.army.mil/ForecastData/GLBasinConditions/LTA-GLWL-Graph.pdf). Due to a strong correlation between water levels and incident wave energy in Lake Michigan (Meadows et al., 1997; Huang et al., 2021), large waves and significant coastal erosion have been reported along many shorelines (Huang et al., 2021; Troy et al., 2021). Zhu et al. (2024) demonstrated, using a coupled wave-current-sediment model, that basin-wide coastal sediment loss in southern Lake Michigan has dramatically accelerated over the past decade due to intensified waves associated with rising water levels. However, at the regional scale, coastal sediment loss has decreased in the western lake while increasing in the eastern lake, influenced by the

* Corresponding authors at: Great Lakes Research Center, Michigan Technological University, Houghton, MI 49931, United States (L. Zhu and P. Xue).
E-mail addresses: lzhu7@mtu.edu (L. Zhu), pexue@mtu.edu (P. Xue).

[1] Given their role as Guest Editors, Pengfei Xue, Longhuan Zhu, and Guy Meadows had no involvement in the peer-review of this article and has no access to information regarding its peer-review. Full responsibility for the editorial process for this article was delegated to Chin H. Wu, Ph.D.

https://doi.org/10.1016/j.jglr.2024.102499
Received 6 May 2024; Accepted 24 November 2024

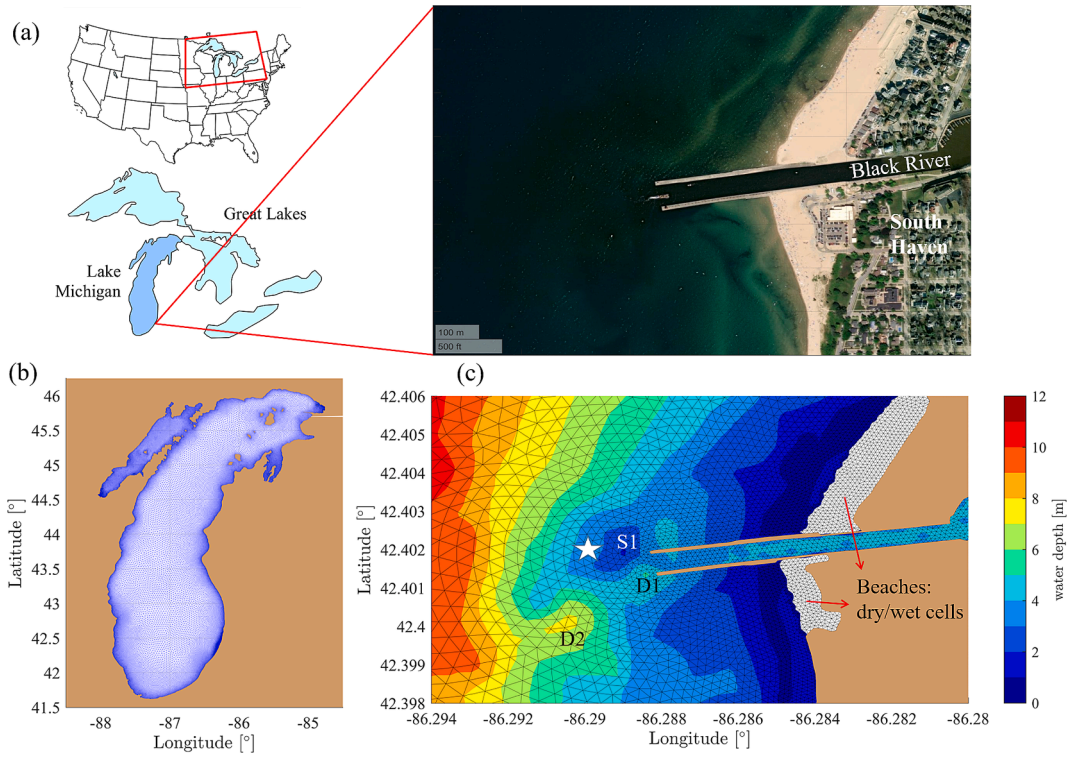

Fig. 1. (a) Location of the study site. Satellite image.
Source: Google Earth. (b) Unstructured triangular mesh for the entire Lake Michigan. (c) A finer mesh of ~10 m for the region near the jetties, where S1 indicates shallow water, D1 and D2 indicate deep waters, and the white star marks the location for the analysis of wind, wave, and current conditions in Section 3.1 and Fig. 9

spatial patterns of wave climate changes. These spatial characteristics underscore the importance of regional analyses in understanding coastal erosion and its association with local wave-current conditions and bathymetry.

On a local scale, coastal erosion is significantly influenced by structures such as offshore breakwaters, jetties, and groins. These structures alter wave and current patterns in adjacent areas, affecting sediment resuspension, transport, and redistribution. This often results in updrift accretion and downdrift erosion (Saengsupavanich, 2019). In Lake Michigan, a common feature is the jetty, a structure built perpendicular to the shoreline to prevent longshore sediment deposition at river mouths. While jetties protect navigation channels from accretion by intercepting longshore sediment transport, they typically cause sediment deposition upstream and erosion downstream (Garel et al., 2015; Flor-Blanco et al., 2015; Wang et al., 2022). While the accreted side may widen beaches and boost the development of beach-related businesses, the eroded side can damage land and property and adversely affect livelihoods. Along with the concurrent deposition updrift and erosion downdrift caused by submerged breakwaters, numerous researchers have observed various patterns of beach morphological changes (Saengsupavanich, 2019; Thiruvenkatasamy and Baby Girija, 2014), though the mechanisms behind this phenomenon are not yet fully understood. Therefore, comprehending local sediment transport and budget near jetties is crucial for effective coastal management, including sediment dredging, nourishment, and ensuring beach safety.

The objective of this study is to investigate the impact of jetties on nearby sediment transport and budget. The focus is on a mid-sized navigational jetty situated in South Haven, MI, on Lake Michigan. For this analysis, medium-sized harbor jetties are defined as those extending offshore to the second sandbar, where they significantly influence sediment transport. This scenario is typical of many recreational and

Table 1
Sediment parameters used in the model.

	Fine sediment	Coarse sediment
Mean sediment diameter D_{50} [μm]	15	150
Fraction	17 %	83 %
Sediment density ρ_s [kg/m^3]	2650	2650
Sediment settling velocity ω [mm/s]	0.2	14.8
Surface erosion rate E_0 [kg/m^2/s]	1.22×10^{-6}	1.31×10^{-4}
Critical shear stress for erosion τ_{ce} [Pa]	0.05	0.15
Critical shear stress for deposition τ_d [Pa]	0.04	0.10

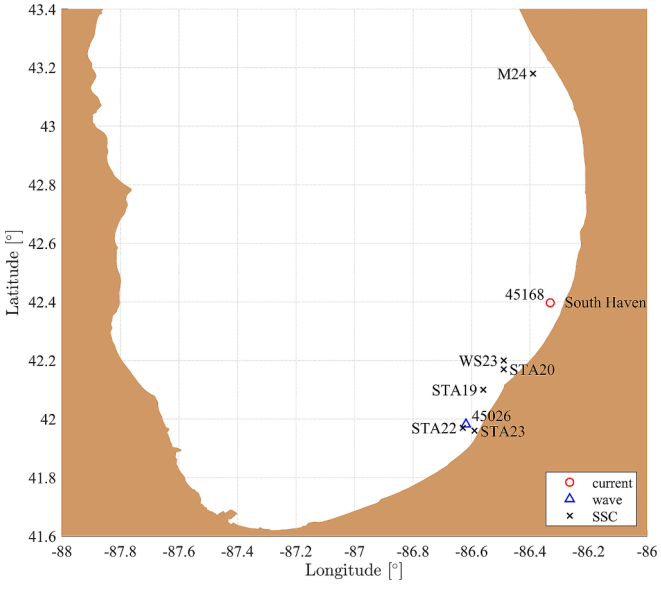

Fig. 2. Locations of the measured data for currents (red circle), waves (blue triangle), and suspended sediment concentration (SSC, black crosses) near the jetties at South Haven.

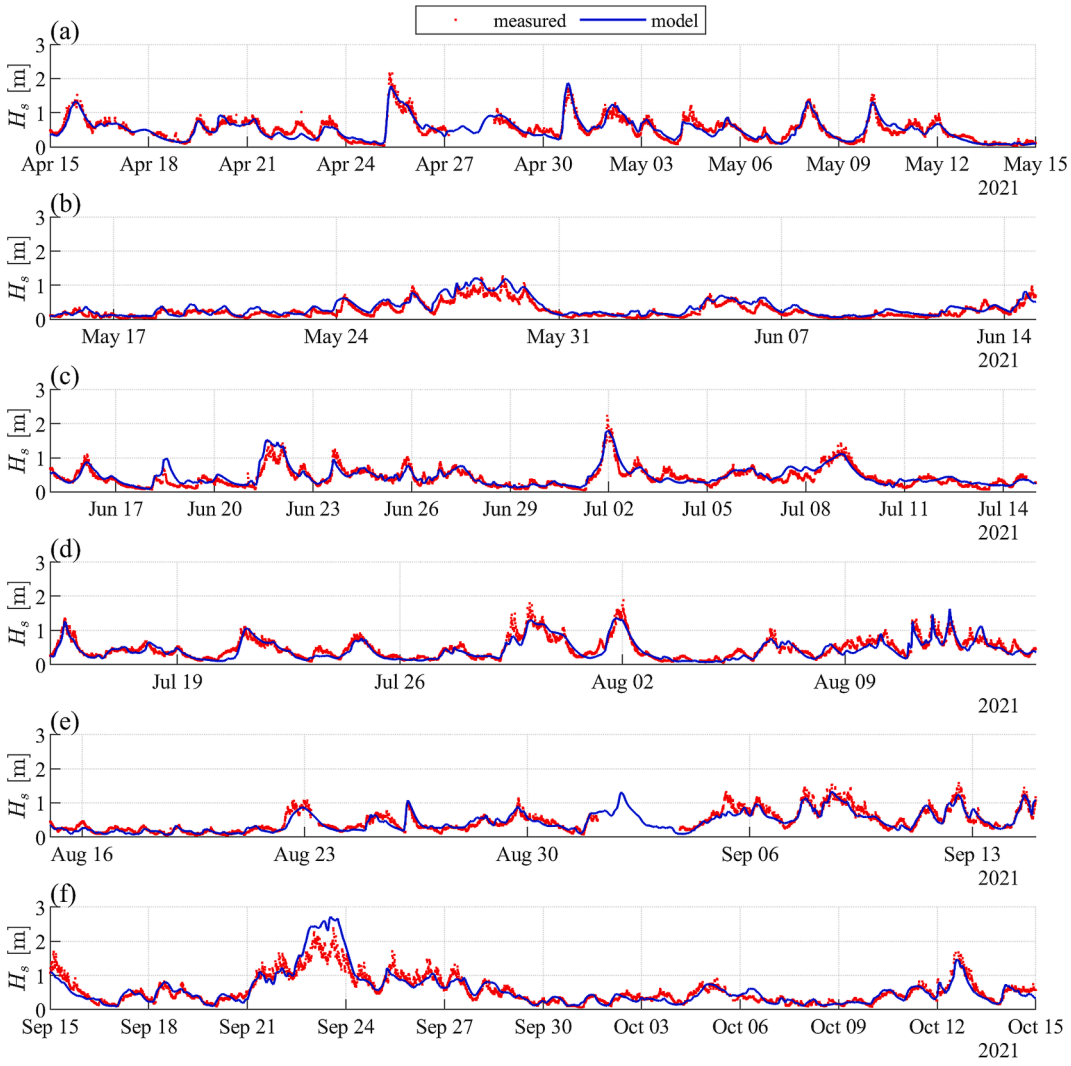

Fig. 3. Comparisons between the modeled (blue lines) and measured (red dots) significant wave height (H_s) at buoy 45168.

refuge harbors along the Great Lakes. The wave-current-sediment processes in the entire lake in the year 2021 are modeled using a coupled model with a very high resolution of approximately 10 m in the region of our interest. Two storm events, characterized by differing wave and current directions at the jetty mouth, were selected to examine the characteristics of sediment transport and budget. Furthermore, sediment transport and budget for the entire navigation season are investigated. These results are also qualitatively verified by two independent "sea truth" surveys conducted in the fall of 2021.

2. Methods

2.1. Study site

In this study, we focus on the coastal region covering the pair of jetties along the city of South Haven, MI, which is located along the southeastern shore of Lake Michigan (Fig. 1a). The selected jetties at the mouth of the Black River in South Haven were first built in 1861 and improved by the Army Corps of Engineers at the end of the 19th century (https://www.terrypepper.com/lights/michigan/southhaven/southaven.htm). The overall lengths of the northern jetty and southern jetty are 1,594 feet (~595.6 m) and 1,554 feet (~473.7 m), respectively, with about 470 feet (~143.2 m) projecting beyond the natural shoreline to the landward side (Fig. 1a). Thus, the jetty length in the water is about 200 to 350 m, considering water level fluctuations. The jetties terminate at the position of the second sandbar (Fig. 1a) and are characterized as medium-sized harbor jetties. The bathymetry is complicated in the immediate vicinity of the jetties, with a shallow area (S1, Fig. 1c) at the lakeward end of the north jetty and deep regions (D1 and D2, Fig. 1c) to the southwest of the jetty.

To maintain the federal navigation channel, the sand and sediment are often removed from the harbor and placed in the eroded region near the jetties in the lake. As a medium-sized structure, the jetties alter the sediment transport and morphology significantly and therefore influence the selection of the places to deposit the sediment dredged from the harbor.

2.2. Model configuration

To investigate the effects of the South Haven jetty on sediment transport and budget, we used the 3D wave-current-sediment model, SWAN-FVCOM-CSTMS (Zhu et al., 2024), which coupled the third-generation wave spectral model, Simulating Wave Nearshore (SWAN, Booij et al., 1999), the ocean circulation model, Finite-Volume Community Ocean Model (FVCOM, Chen et al., 2003), and the sediment transport model, Community Sediment Transport Modeling Systems (CSTMS, Warner et al., 2008). The computational domain covering the entire lake was developed using an unstructured triangular mesh with bathymetry and shoreline datasets from the National Oceanic and Atmospheric Administration (https://www.ngdc.noaa.gov/mgg/great

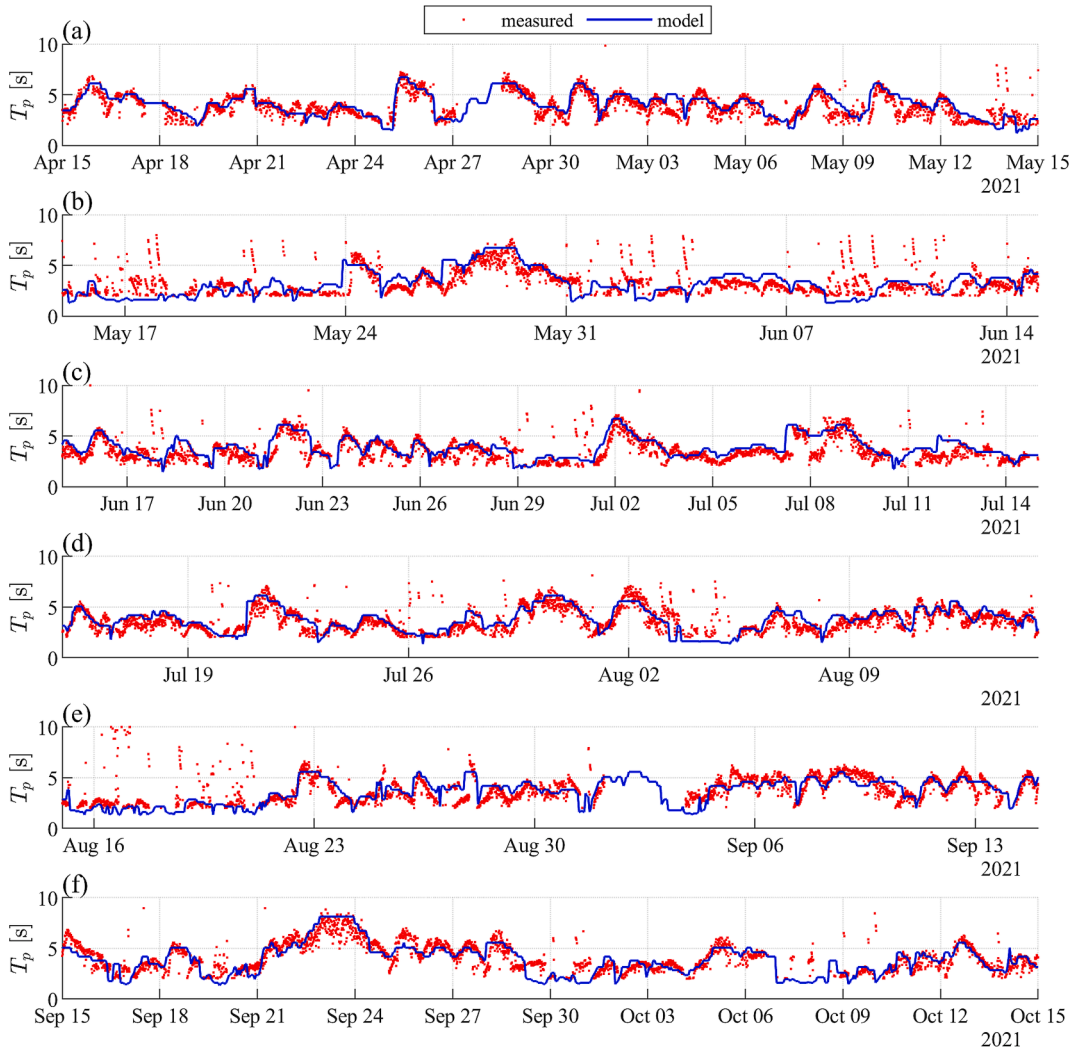

Fig. 4. Comparisons between the modeled (blue lines) and measured (red dots) peak wave period (T_p) at buoy 45168.

lakes/michigan.html). The horizontal resolution of the mesh varied from ~ 60–300 m near the coast to ~ 4.4 km in the central lake areas (Fig. 1b). To resolve the jetty, the mesh near the jetty was refined to ~ 10 m based on the nearshore bathymetry data (Fig. 1c), which is a combination of 2012 USACE NCMP Topobathy Lidar data from NOAA Digital Coast: Access Viewer (https://coast.noaa.gov/dataviewer/#/lidar/search/) and data from the NOAA Office of Coast Survey (https://encdirect.noaa.gov/). The computational grids for the beaches on both sides of the jetty dynamically adjust in response to water level changes by characterizing the grid cells as either wet or dry. Cells submerged in water are marked as wet, while exposed cells are marked as dry. These designations change as water levels rise or fall, and only wet cells are used in hydrodynamic computations. The vertical direction was discretized into 20 sigma layers such that the vertical resolution was ~ 0.05 m near the coast and less than 5 m for most offshore regions. The vertical mixing processes and the horizontal diffusivity were calculated using the Mellor-Yamada level-2.5 (MY25) turbulence closure model (Mellor and Yamada, 1982) and the Smagorinsky numerical formulation (Smagorinsky, 1963), respectively. The horizontal and vertical mixing coefficients are 0.1 and 10^{-5}, respectively, which are the default values. The default bottom roughness length scale is 0.002 with the minimum bottom roughness of 0.0025.

The sediment properties were reasonably estimated based on previous studies and model calibration. Since most of the suspended sediment is finer than the surficial bottom sediment (Eadie and Lozano, 1999), Lou et al. (2000) set the grain size (D_{50}) at 30 μm as a representative for the entire lake. However, the model with a single grain size class may not work well for more than one location (Cardenas et al., 2005). Thus, Cardenas et al. (2005) used two sediment classes, with one for fine sediment and the other for coarse sediment. Additionally, Hawley et al. (2009) tried four sediment size classes, and Khazaei et al. (2021) used six sediment size classes. However, Hawley et al. (2009) pointed out that the results using two size classes were similar to those with four size classes. Therefore, two representative sediment classes with 15 μm for fine sediment and 150 μm for coarse sediment were used in this study. The fraction of each sediment class is estimated based on the sediment percentage in the coastal area of Lake Michigan (Eadie and Lozano, 1999) and adjusted based on the model calibration. The estimated sediment sizes were also comparable to the ones used in Hawley et al. (2009) and Khazaei et al. (2021). The sediment density was set using the default value of 2650 kg/m^3 (Soulsby, 1997), which is comparable to the estimations (2300–2450 kg/m^3) in Khazaei et al. (2021). With the grain size, sediment density, and water viscosity, the settling velocity (ω), surface erosion rate (E_0), and critical shear stresses for erosion (τ_{ce}) and deposition (τ_d) can be calculated based on the formulas in Soulsby (1997) with the code available through https://github.com/pwcazenave/fvcom-toolbox/tree/master/utilities. The calculated surface erosion rate was adjusted for a better comparison between measured and modeled suspended sediment concentration (SSC). The details of the sediment properties are summarized in Table 1. The Black River

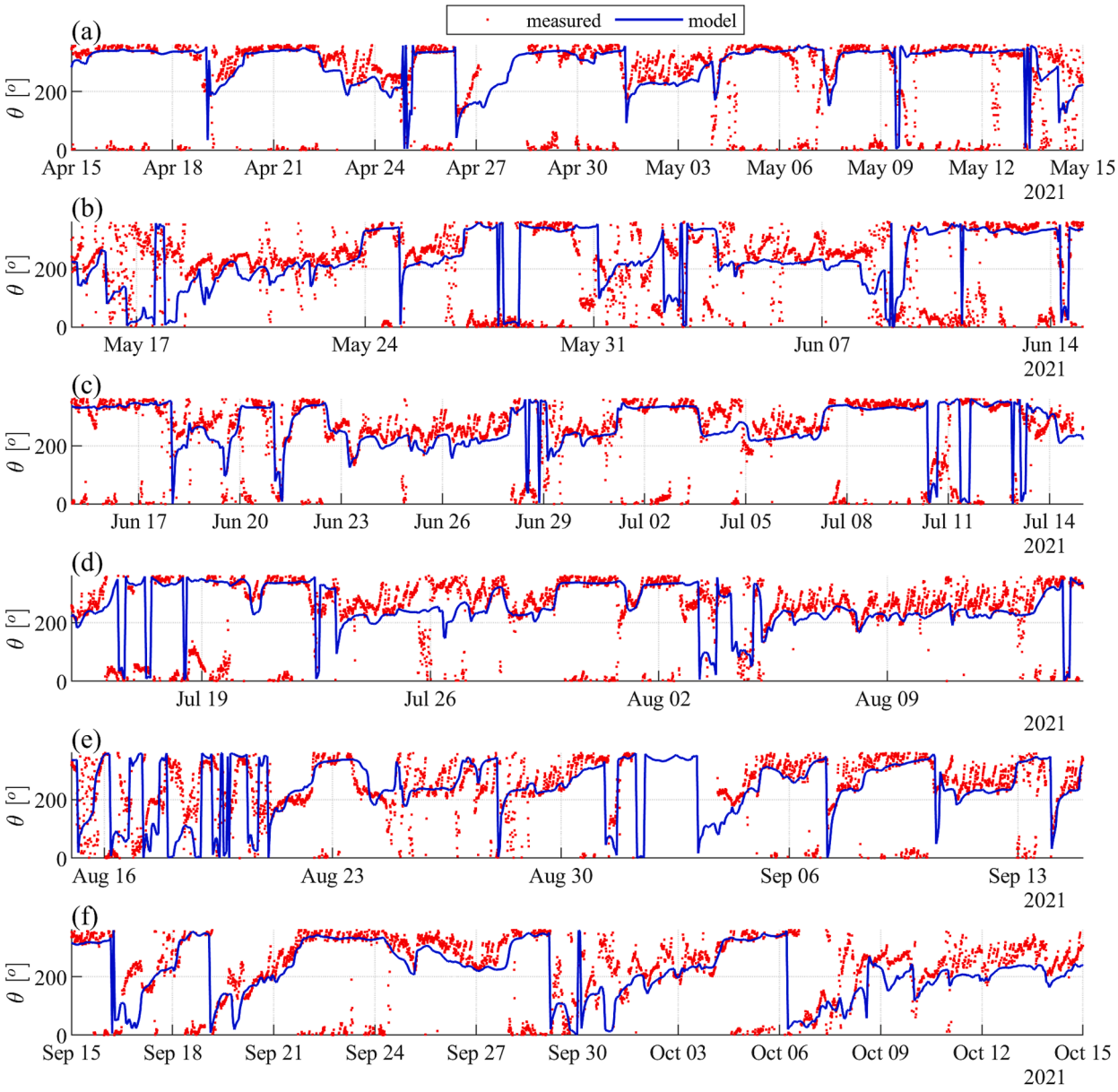

Fig. 5. Comparisons between the modeled (blue lines) and measured (red dots) dominant wave direction (θ) at buoy 45168. The wave direction is where the waves at the dominant period come from, which increases clockwise, with 0 degrees from true north and 90 degrees from east.

discharge was estimated based on historical data at the south branch (USGS 04102700) and middle branch (USGS 04102776) with the data available from USGS water resources (https://waterdata.usgs.gov/nwis/). Due to the lack of reliable data on sediment supply from the river, we assumed no sediment contribution from this source. While this assumption may result in an underestimation of the sediment budget around the jetties, it does not affect the analysis of jetty-induced changes during storm events. In fact, it helps isolate the jetties' influence on coastal sediment transport, independent of land-based sources. The driving forces, including wind forcing and surface heat fluxes, were interpolated from the hourly datasets from the High-Resolution Rapid Refresh (HRRRv2, https://rapidrefresh.noaa.gov/hrrr/), which is a real-time 3-km resolution, hourly updated, cloud-resolving, convection-allowing atmospheric model from NOAA, initialized by 3 km grids with 3 km radar assimilation. HRRR outputs have been designated as surface forcing for the NOAA Great Lakes Operational Forecasting System. The water level was updated monthly based on the monthly mean water level data (https://www.lrd.usace.army.mil/Water-Information/Water-Management/Great-Lakes-and-Harbors/Water-Level-Data/).

2.3. Model validation

To validate the model, the model results were evaluated against the measured waves at buoy NDBC 45168 and the measured currents at buoy NDBC 45026 near the jetties from the National Data Buoy Center (https://www.ndbc.noaa.gov/). The buoys were installed in April and pulled out in November 2021 to avoid damage from ice, which usually occurs from December to March. As no sediment transport data were available for 2021, we used historical suspended sediment concentration (SSC) data available from 1994, 1998, and 2002, collected at nearby locations, to validate the sediment transport model. The SSC datasets are from the project Episodic Events: Great Lakes Experiment (EEGLE, https://www.glerl.noaa.gov/res/projects/eegle), Lou et al. (2000), and Lee et al. (2005). The locations for the measured data are shown in Fig. 2.

The model-data comparisons for significant wave height (H_s), peak wave period (T_p), and dominant wave direction (θ) at buoy 45168 are

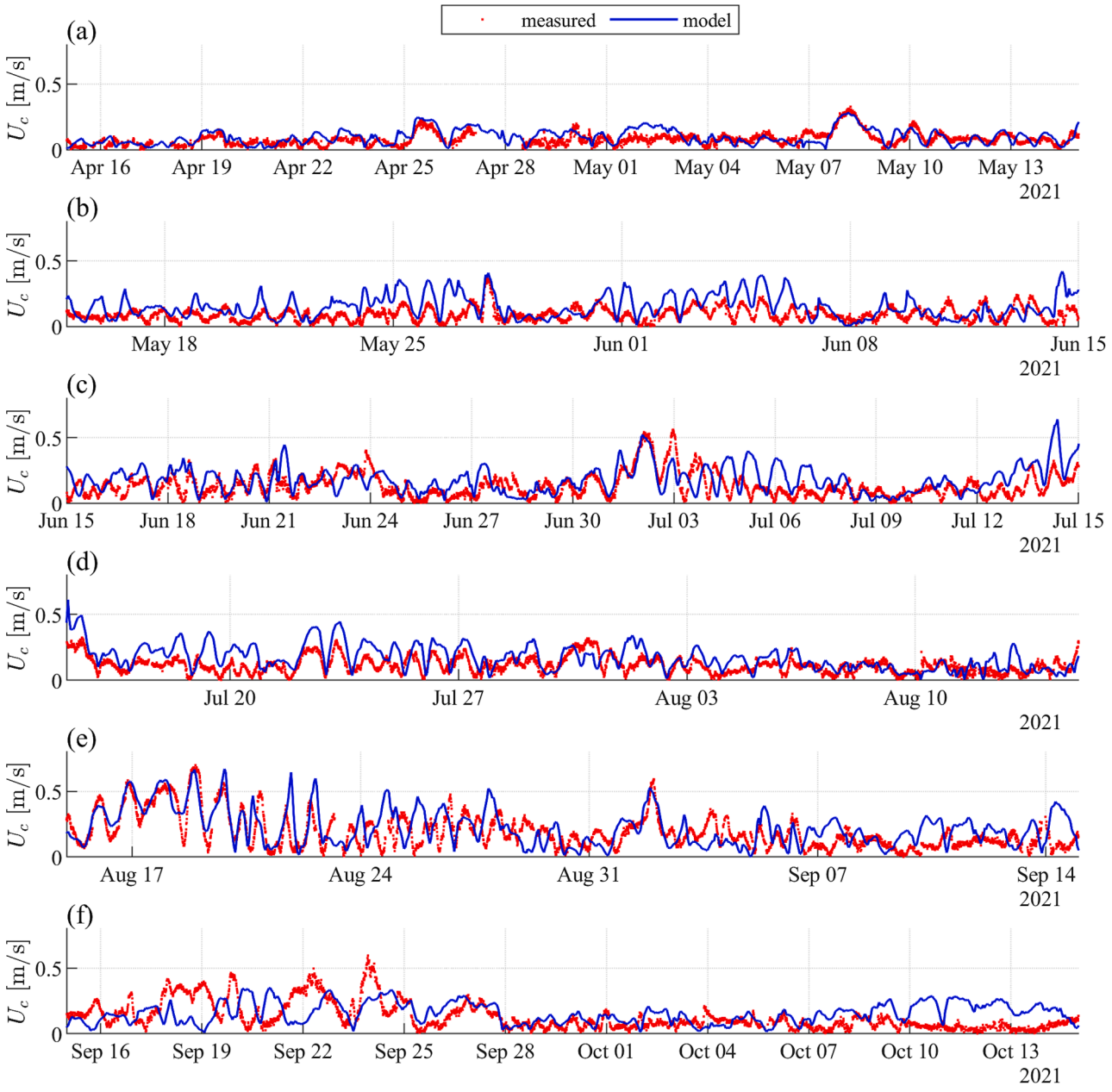

Fig. 6. Comparisons between the modeled (blue lines) and measured (red dots) current speed (U_c) at 1 m deep at buoy 45026.

shown in Figs. 3, 4, and 5, respectively. The model not only captures the storm waves but also shows good agreement with the observation of small waves. Although there are small discrepancies for some time (e.g., September 23 in Fig. 3f), the model performs well in most cases. As shown in Fig. 4, the model performs well in the simulation of the peak wave period too. For the dominant wave direction, the model also compares well with the observation by capturing the temporal patterns of θ. Overall, the model results are in good agreement with the measured data for wave comparison.

The model performance in the current simulation is demonstrated by comparing the model current velocities with the observations at buoy 45026 (Figs. 6 and 7). Similar to the wave simulation, the model captures well the spatial pattern of the current with an overestimation of the current speed for some time. In general, the model matches well with the current direction most of the time. Thus, overall, the model and the observations generally compare well.

The effectiveness of the model in simulating sediment transport is assessed through the comparison between the modeled and measured suspended sediment concentration (SSC) as illustrated in Fig. 8. Though sediment models are generally known to be less precise compared to wave and hydrodynamic models, our modelled SSC reasonably reproduces the observed patterns, with an R^2 ranging from 0.39 to 0.77 (Fig. 8) except the location STA20 with a low R^2 value of 0.05 in 1998 (Fig. 8e). Despite this low R^2 at this site, the model still captured major SSC events, such as the events on November 11 and December 23, 1998. In 1999, the model at this site performed relatively better, with an R^2 of 0.39 (Fig. 8g). Overall, there is good agreement between the modeled SSC and the observed data.

The validated model was then used to study sediment transport and budget around the jetty at South Haven. To investigate the effects of the jetty, scenarios without the jetty were also conducted for comparison. In the scenarios without jetty, the bathymetry in the channel was smoothed out to improve the model stability when removing the jetty, while the bathymetry out and around of the channel did not change. Although the jetties can also influence sediment transport indirectly by changing the

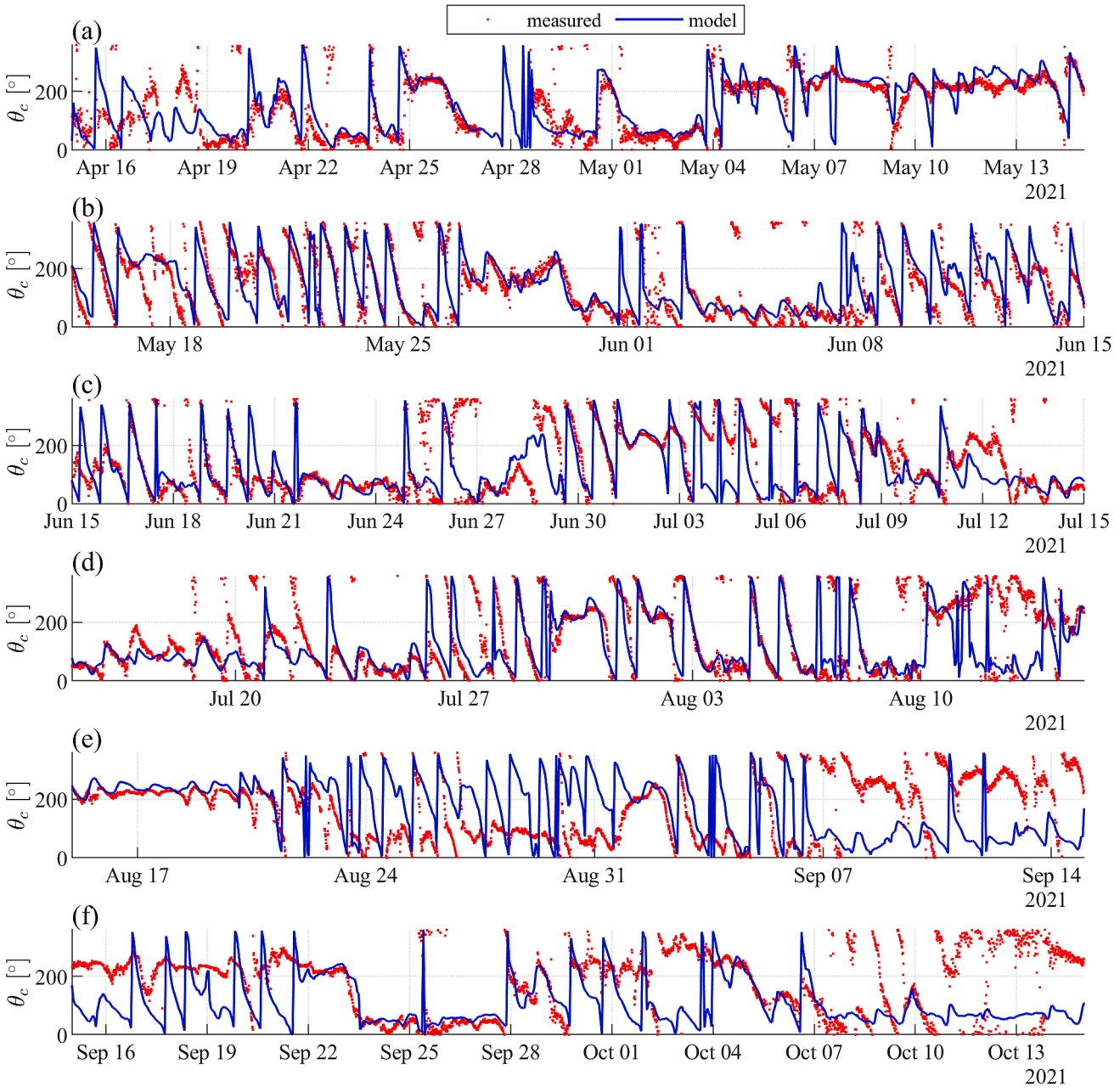

Fig. 7. Comparisons between the modeled (blue lines) and measured (red dots) current direction (θ_c) at 1 m deep at buoy 45026. The current is toward the east at 0 degrees and toward the north at 90 degrees.

bathymetry around the jetties in the long term, the purpose of this study is to show the direct effects of the jetties on the sediment transport under storm events. Therefore, the bathymetry around the jetties is not changed with the benefits to identify the direct influences of the jetties on sediment transport.

3. Results and Discussion

3.1. Wind, wave, and current conditions

Since Lake Michigan may be partially frozen from December to April (Huang et al., 2021), we focus on the ice-free navigation season from April 1 to December 1 in 2021 in this study. The wind, wave, and current roses for the selected location at the jetty mouth (Fig. 1) are shown in Fig. 9. During the period from April 1 to December 1, the waves and currents were predominantly directed to the north and south. The waves propagated from offshore and the current flowed along the coast. The mean and maximum wind speeds were 4.73 m/s and 16.57 m/s, respectively. The mean and maximum wave heights were 0.50 m and 2.02 m, respectively. The mean and maximum depth-averaged current speeds were 0.11 m/s and 0.75 m/s, respectively.

To explore the sediment transport and budget under different wind, wave, and current conditions, we selected two representative storm events with distinct directions of wave and current (Fig. 9). Event 1 occurred from 09/22 17:00 (UTC) to 09/24 02:00 (UTC) with waves and currents from the north. During event 1, the wave height ranged from 1.58 m to 2.00 m with an average of 1.90 m. The wave period ranged from 7.40 s to 8.14 s with an average of 8.05 s. The depth-averaged current speed ranged from 0.43 m/s to 0.75 m/s with an average of 0.66 m/s. Event 2 occurred from 11/11 20:00 (UTC) to 11/13 05:00 (UTC) with waves and currents from the south. During event 2, the wave height ranged from 1.36 m to 1.88 m with an average of 1.69 m. The

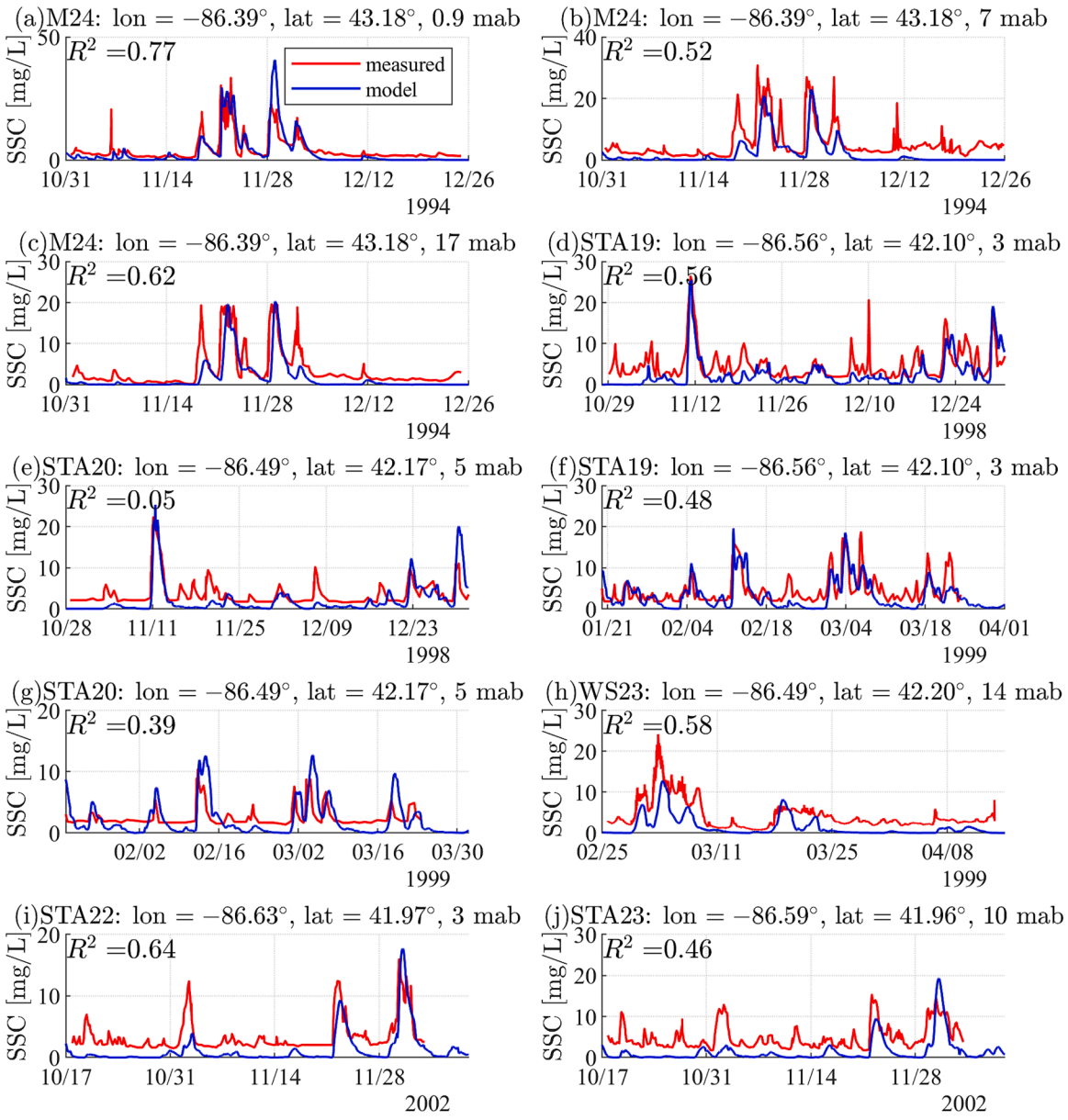

Fig. 8. Comparisons between modeled (blue lines) and observed (red lines) suspended sediment concentration (SSC) at the stations M24 (1994), STA19 (1998, 1999), STA20 (1998, 1999), WS23 (1999), STA22 (2002), and STA23 (2002).

wave period ranged from 5.56 s to 6.73 s with an average of 6.12 s. The depth-averaged current speed ranged from 0.35 m/s to 0.60 m/s with an average of 0.47 m/s. The waves and currents in event 2 were smaller than those in event 1. Both storm events lasted 33 h.

3.2. *Sediment resuspension and morphodynamics in storm events*

The sediment resuspension and the resulting morphological erosion under the two representative storm events are shown in Fig. 10. As water depth decreased toward the shoreline, the waves break as they approach the nearshore, yielding smaller and smaller wave heights (Fig. 10a). The effects of the jetties on waves are limited to a small region around the jetties (Fig. 10a and c). In contrast, the currents are more significantly influenced by the jetties, resulting in much higher velocities near the mouth of the jetty and much lower velocities in the downstream direction (Fig. 10b1 and b3). The sediment resuspension is induced by combined waves and currents. Although the suspended sediment concentration near the bottom (SSCb) is more correlated with the wave bottom velocity (Fig. 10d and c), the effects of currents are not ignorable, especially with the presence of jetties, which changes the current significantly. The effects of the jetties on SSCb are more significant in event 1 with stronger waves and currents from the north compared to event 2 with dominant forcing from the south (Fig. 10d). In event 1, the currents are enhanced at the mouth of the jetties and remain at a large value for several kilometers downstream, such that the associated SSCb is higher in these regions (Figs. 10b1-2 and d1-2). Similarly, the reduced currents behind the south jetty result in smaller SSCb (Figs. 10b1-2 and d1-2). In event 2, with waves and currents from the south, the SSCb increases at the mouth of the jetty associated with increasing currents as expected. However, the SSCb behind the north jetty in the downstream direction also increases, which is probably induced by the large velocity along the north jetty due to the strong eddy induced by the jetty (Fig. 10b3). The effects of the jetties on waves, currents, and sediment resuspension yielded significant influences on morphological erosion, which is further complicated by bathymetric variance (Fig. 10e). However, the influences of the jetties on these individual storms are limited

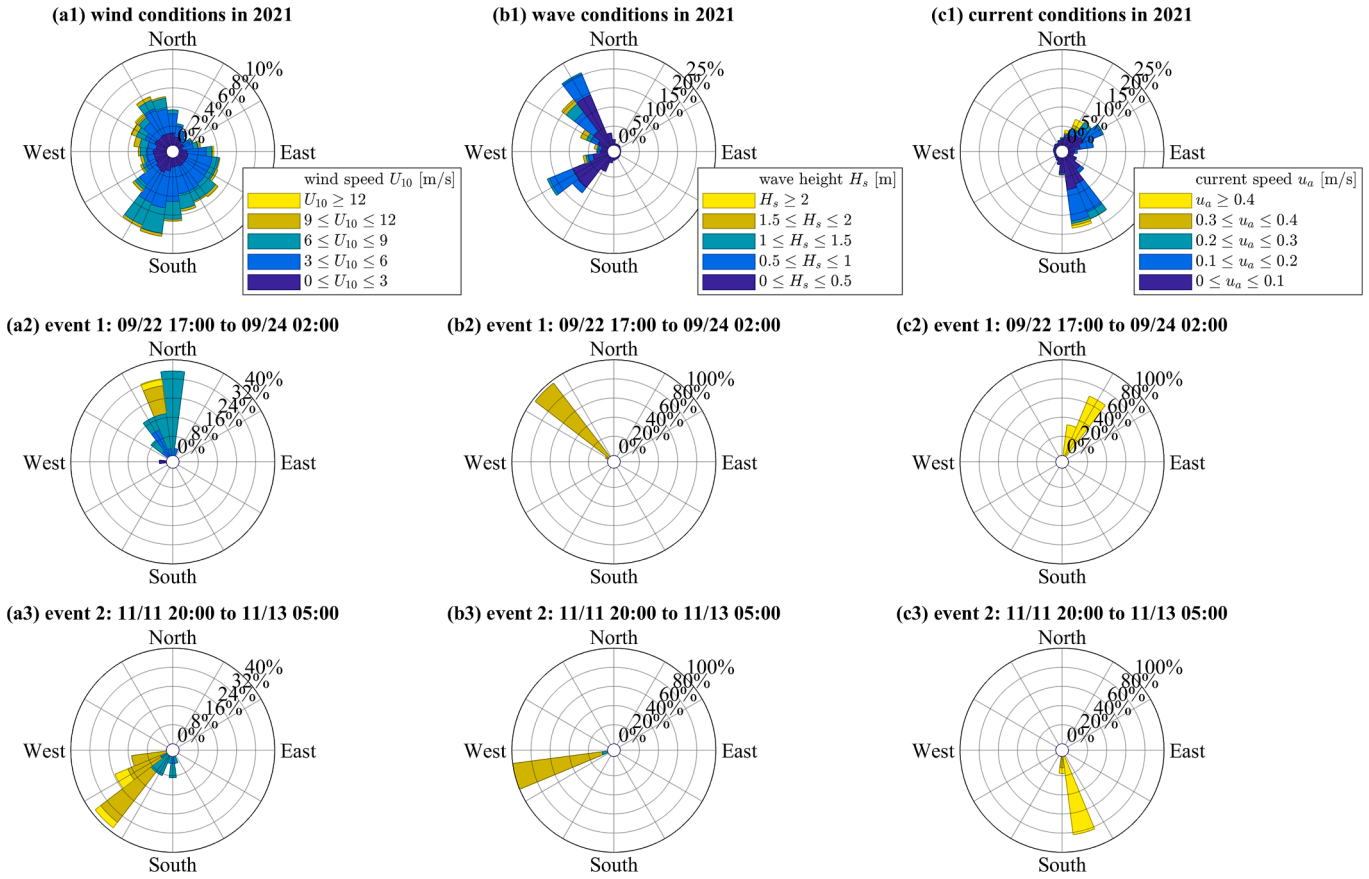

Fig. 9. Wind (column a), wave (column b), and depth-averaged current (column c) roses at the mouth of the jetties from April 1 to December 1 in 2021 (row 1), in event 1 from 09/22 17:00 to 09/24 02:00 (row 2) and in event 2 from 11/11 20:00 to 11/13 05:00 (row 3). The directions are where the wind, wave, and current come from. The time is Coordinated Universal Time (UTC). The location for these data is marked in Fig. 1c.

to a smaller region around the jetties. We therefore concentrated on this specific area to investigate the mechanisms underlying the effects of the jetties on morphological dynamics, in relation to variations in bathymetry (Fig. 11).

In event 1 without the jetties, high SSCb occurs in the region with a water depth of 3–5 m around the jetties (Fig. 11b1), especially in the shallow water S1 at the mouth of the jetties. The regions D1 and D2 are deeper resulting in lower SSCb. As the water flows directly southward without the jetties, the sediment eroded in shallower regions is carried southward and deposited in deeper areas such as D1 and D2 adjacent to the shallower area S1 (Fig. 11b2). With the presence of the jetties, the currents are significantly changed. The currents are converged and enhanced at the mouth of the jetties (e.g., S1 and D2 in Fig. 11a2). A small anticlockwise eddy is generated on the north side of the jetties with currents flowing toward the shore along the north jetty. On the south side of the jetties, there is a large anticlockwise eddy with strong currents flowing offshore along the south jetty. The currents and waves are weaker at both sides of the jetties, resulting in lower SSCb (Fig. 11a1 and a2). However, the SSCb at the jetty mouth (more southward) is higher due to accelerated currents (e.g., D2 in Fig. 11a1). As the currents increase at the jetty mouth, the erosion at S1 increases significantly with the sediment transported southward. In addition, the sediment along the north jetty is eroded by the strong currents but limited to a very small region adjacent to the jetty. The sediments eroded at the mouth are mainly deposited in the deep region D2 carried by the currents.

In event 2, without the jetties, the currents flowed toward the north unobstructed (Fig. 11d2). With the presence of the jetties, the currents are converged toward the jetty mouth and enhanced at the mouth (Fig. 11c2). On the north side of the jetty, there is a clockwise eddy yielding strong currents offshore along the north jetty. The sediment erosion is significant in the shallow region S1. With the presence of the jetty, the erosion at S1 is more significant due to stronger currents at the jetty mouth. At the deeper regions D1 and D2, there is no significant difference in the morphological erosion between the scenarios with and without the jetties. This is different from the scenarios in event 1, indicating that the impact of the jetties is heavily dependent on the directions of the waves and currents, which is possibly due to the asymmetric bathymetry on both sides of the jetties.

3.3. *Sediment transport and budget*

To explore the effects of the jetties on the longshore sediment transport, the transport is calculated along the shore with and without the jetties (Fig. 12a1-3). Transect lines are constructed perpendicular to the shoreline at approximately 100 m intervals along the ~ 4000 m-long coast. The sediment transports calculated from two lengths of transect lines (in the offshore direction) of 500 m and 800 m are compared in Fig. 12.

In event 1, with waves and currents from the north, the sediment transport is southward (negative value in Fig. 12). The sediment transport decreases significantly on the downstream (south) side of the jetty, especially for the 500-m transect lines, due to the reduction of current (Fig. 12.a1, b1, and c1). The sediment transport restores after ~ 1200 m (~5 times the length of the portion of the jetty that is in the water) downstream of the jetty, indicating that the effects of the jetties for individual storms are limited to a small region along the shore. The smaller difference between the sediment transport through wider transect lines (800 m) with and without the jetty also demonstrates that the influence of the jetty is limited to a small region across the shore. In event 2, with waves and currents from the south, the sediment transport is northward.

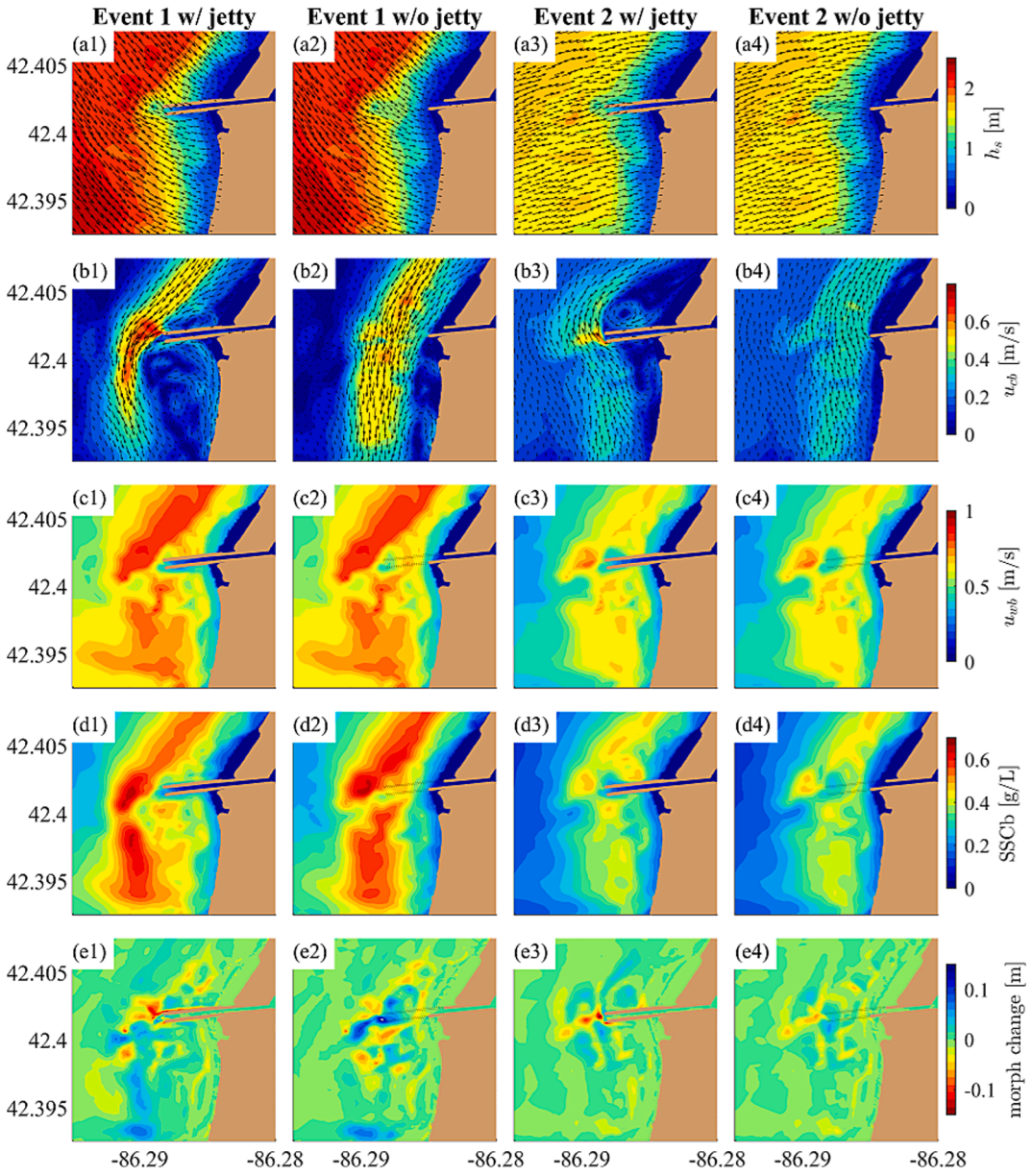

Fig. 10. Comparisons between the wave height (h_s, row a), bottom current velocity (u_{cb}, row b), bottom wave orbital velocity (u_{wb}, row c), bottom suspended sediment concentration (SSCb, row d), and morphological erosion (row e) near the jetty in event 1 from 09/22 17:00 to 09/24 02:00 (column 1 with jetty and 2 without jetty) with winds primarily from the north and north-northwest (Fig. 9a2) and event 2 from 11/11 20:00 to 11/13 05:00 (column 3 with jetty and column 4 without jetty) with winds primarily from the southwest (Fig. 9a3). The time is UTC.

For this storm condition, sediment transport also decreases on the downstream (north) side of the jetty. However, the reduction of sediment transport is much smaller than that in event 1, probably due to the smaller waves and currents, and the smaller eddy associated with currents on the north side of the jetty.

For the entire navigational period (April 1 to December 1), the cumulative sediment transport is southward, although the mean offshore circulation is anticlockwise (Beletsky and Schwab, 2008; Xue et al., 2017). This is because sediment transport is mainly determined by storm wave events in the nearshore region. During stormy times when the significant wave height at the jetty mouth is greater than 1 m, the current is southward. As the storm currents are southward, there is a large eddy on the south side of the jetty such that the current adjacent to the jetty is re-circulated northward. Thus, the sediment transport near the south jetty is northward in favor of sediment retention (Fig. 12a3). Overall, the sediment transport decreases significantly on the south side of the jetty for the entire navigational period due to the presence of the jetty. Meanwhile, the sediment transport on the north side of the jetty increases associated with enhanced bottom SSC due to the effects of the jetty (Fig. 10d).

To explore the resulting sediment budget influenced by the jetties, the ~ 800 m-wide and ~ 4000 m-long coastal region were divided into ~ 100x100 m^2 budget cells. A positive sediment budget results from net sediment gain into the budget cell and indicates sediment deposition while negative sediment budget results from net sediment loss and indicates erosion. The budget cells demonstrate deposition and erosion due to the variance of local bathymetry and wave and current conditions. As shown in Fig. 13, in event 1, with waves and current from the north, the erosion accelerated at the jetty mouth due to the acceleration of currents in that location. The budget cells behind the south jetty have sediment deposition because of the eddy (Fig. 12b1). In event 2 with waves and currents from the south, the erosion is accelerated at the

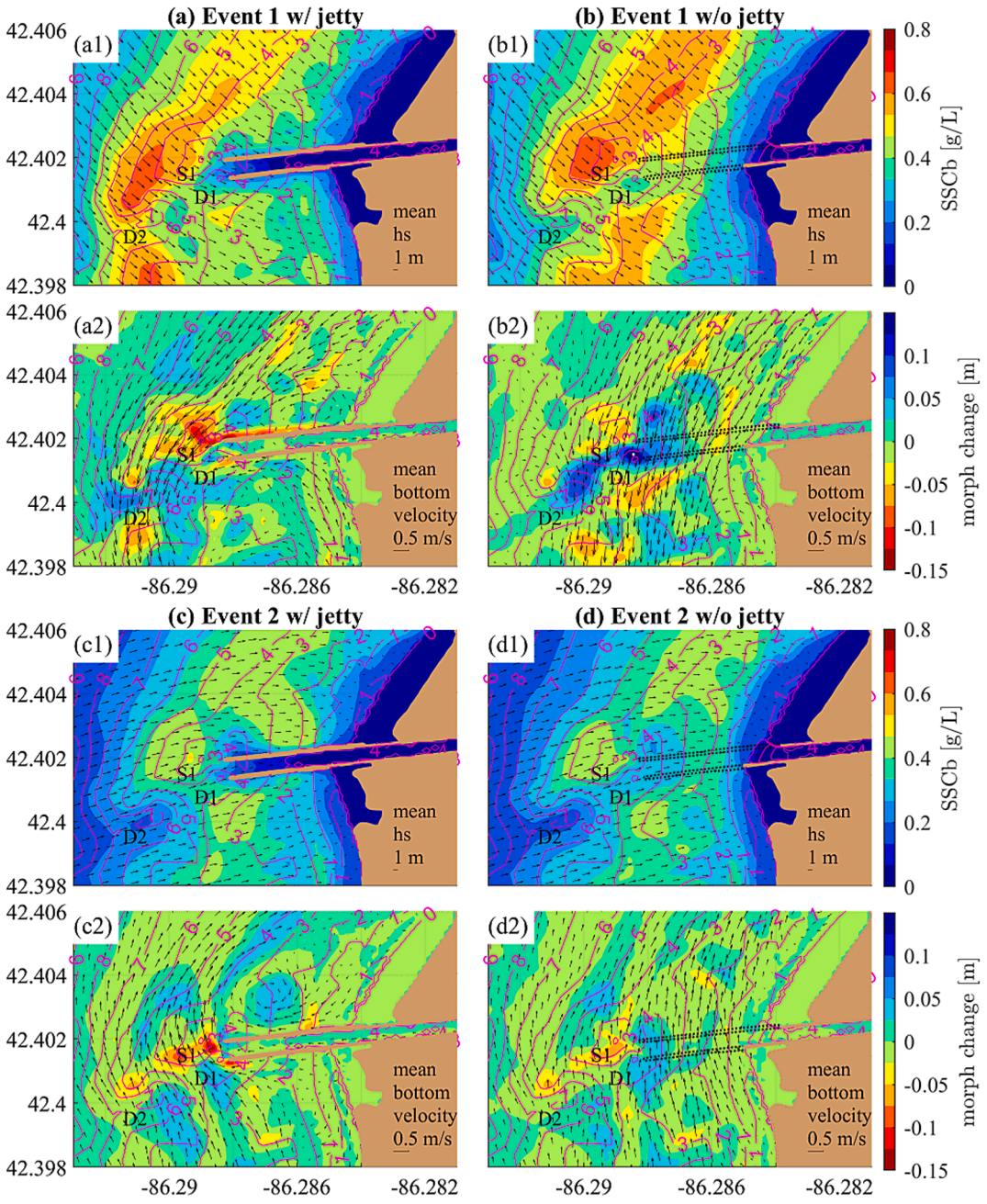

Fig. 11. Directed mean wave height (h_s, arrows), bottom suspended sediment concentration (SSCb, colors), mean bottom velocity (arrows), and morphological erosion (colors) in the two representative storm events: (a) event 1 from 09/22 17:00 to 09/24 02:00 and (c) event 2 from 11/11 20:00 to 11/13 05:00. The time is UTC. The corresponding scenarios without the jetty are shown in (b) and (d), respectively. The bathymetry is denoted by magenta lines with the unit of meter. S1 denotes a shallow water area, while D1 and D2 denote two deep water areas near the jetty.

mouth, with deposition on the north side of the jetties where the jetties prevent the action of waves and currents in the downstream direction.

For the entire navigational period, the deposition accelerates around the jetties, except for the one budget cell adjacent to the jetty mouth (Fig. 13c). However, far from the south jetty in the southerly direction, the erosion exacerbates. Sediment accretion occurs immediately adjacent to the jetties on both sides, which widens the beaches in both fillet regions (Fig. 13c and Fig. 14a). As the storm induced currents flow from the north, the jetties reduce currents on the northern side and also generate a large anticlockwise eddy on the south side of the jetties, the sediment accretion occurs on adjacent regions (fillets) on both sides of the jetties (Fig. 14a). A portion of the gross quantity of sediment being transported southward is recirculated and transported northward to the jetty for deposition by the generation of the eddy. This results in more erosion occurring at the far south of the study region due to reduced sediment supply. Recently, the U. S. Army Corps of Engineers conducted beach nourishment at the South Beach on the southern side of the jetties by placing the sediment dredged from the navigational channel (https://www.mlive.com/public-interest/2023/06/beachgoers-frolic-around-south-haven-harbor-dredging-outwash.html; Fig. 14b-d). The nourishment can enhance the safety of the South Beach. Simultaneously, a portion of the sediment will be carried downstream, serving as a sediment source that helps mitigate erosion in the southern area (Fig. 14a).

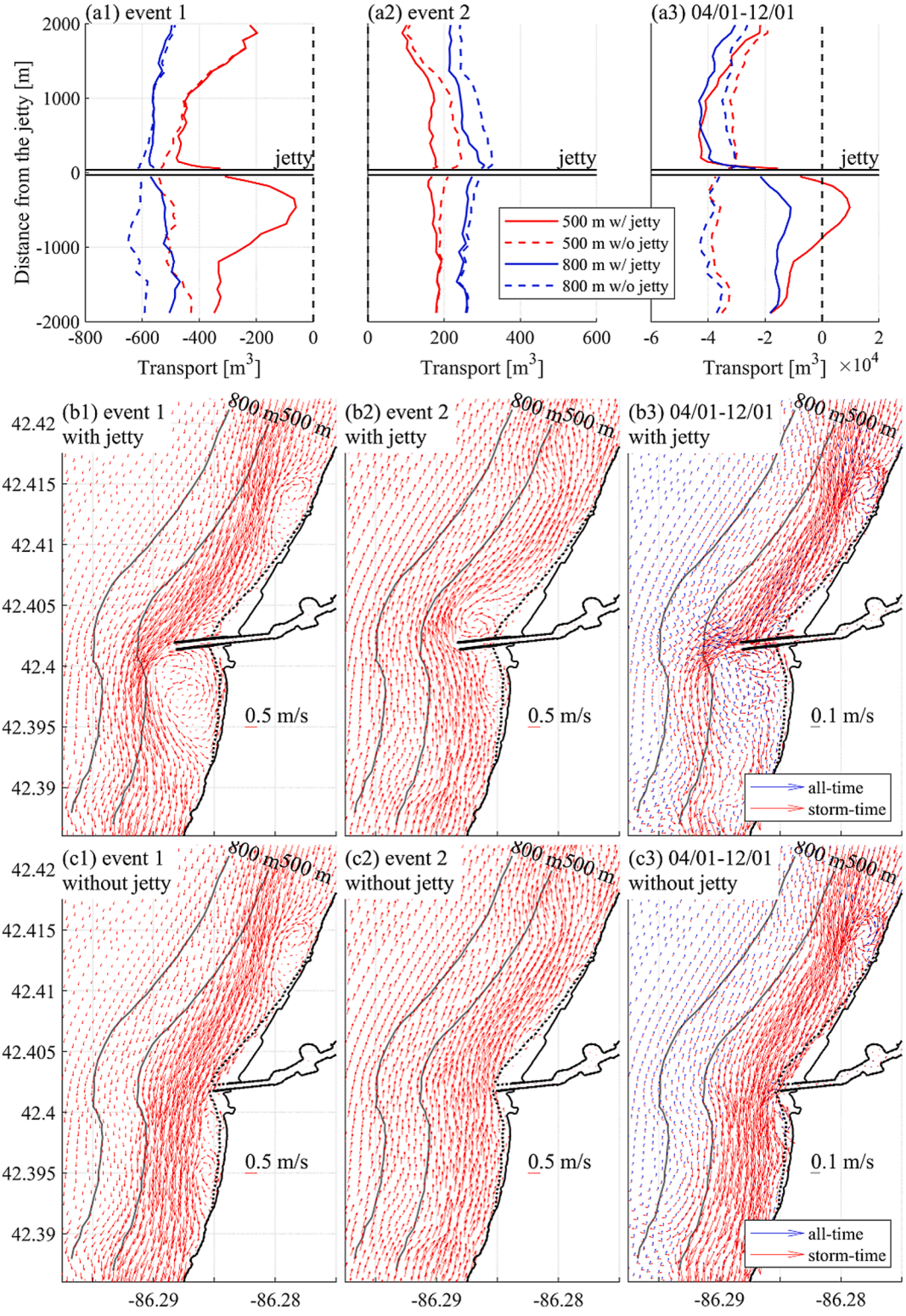

Fig. 12. Alongshore sediment transport during (a1) event 1 from 09/22 17:00 to 09/24 02:00, (a2) event 2 from 11/11 20:00 to 11/13 05:00, and (a3) the whole year from April 1 to December 1. The time is UTC. The sediment transport is calculated from 500 m- (red lines) and 800 m-long (blue lines) transect lines along the shore with an interval of ~ 100 m. The solid lines indicate the transport with the jetties while the dashed lines indicate the transport without the jetty. Positive values indicate northward transport while negative values indicate southward transport. The corresponding mean depth-averaged currents during the events are shown in (b) and (c) for the currents with jetties and without jetty, respectively.

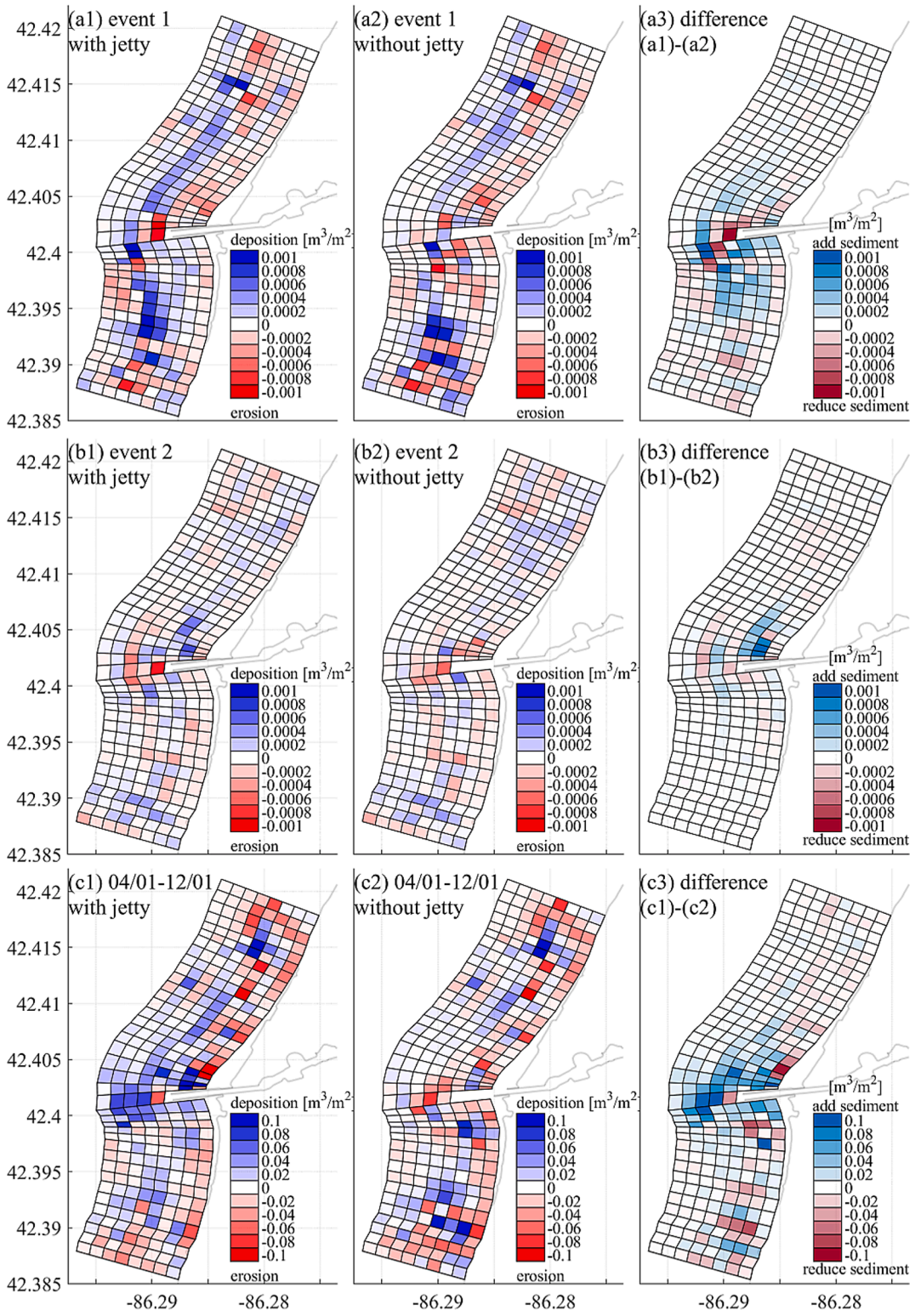

Fig. 13. Sediment erosion and deposition in the budget cells for (a) event 1, (b) event 2, and (c) the whole year (April 1 to December 1). The first column is the results with the jetty and the second column is the results without the jetty, where red indicates erosion and blue indicates deposition. The third column is the difference between the sediment budget influenced by the jetty and without the jetty, where red indicates sediment reduction (erosion acceleration or deposition deceleration), and blue indicates sediment reduction (erosion deceleration or deposition acceleration).

3.4. Qualitative verification

In an effort to provide verification of the simulation provided by the numerical analysis of the sediment transport and sediment budget influenced by a medium-sized harbor jetty in storm events, two independent "sea truth" surveys were conducted. The first was a detailed hydrographic survey conducted in the fall of 2021. This survey was conducted from an instrumented personal watercraft (PWC) from approximately 1 m water depth, offshore to approximately 12 m water depth. Survey profiles were placed at 100-m intervals, perpendicular to

Fig. 14. (a) Sketch for the sediment accretion and erosion near the jetty, where the arrows indicate the dominant direction of the currents (as well as the sediment transport) in storm time and the white area indicates the location for the beach nourishment by U.S. Army Corps of Engineers in August 2022 (https://www.lrd.usace.army.mil/Media/News-Releases/Article/3132077/corps-of-engineers-to-begin-dredging-beach-nourishment-in-south-haven/). (b-d) Beach nourishment on the South Beach in South Haven in June 2023. (b) A hydraulic dredging platform. (c) and (d) Beach nourishment. Photo.
Source: https://www.mlive.com/public-interest/2023/06/beachgoers-frolic-around-south-haven-harbor-dredging-outwash.html

the shoreline and extending approximately 2.0 km to the north of the north harbor jetty and 1.9 km south of the south harbor jetty (Fig. 15a). This range of the survey was designed to capture the full extent of the sediment-rich, updrift fillet as well as the high erosion regions, downdrift fillet. The resulting bathymetry was corrected for transducer offset, water elevation at the time of the survey and rectified to Great Lakes navigational chart datum (IGLD 85). The resulting rectified bathymetry is presented in Fig. 15(b).

In addition to the bathymetric bottom survey in the vicinity of the harbor structures, a detailed autonomous underwater vehicle (AUV), side scan sonar and photographic mission was also completed in the summer of 2021. The goal of this effort was to document the offshore extent of movable nearshore sediment in the harbor region. To complete this underwater survey, an OceanServer, IVER 3, AUV was programed to complete 11 survey lines, three lines at the northern extent for the north fillet, three lines at the southern extent of the downdrift erosion regions, three lines immediately north of the north harbor jetty, and two lines immediately south of the south jetty (Fig. 16). These four sets of underwater survey lines were also conducted on 100 m spacing and were approximately 1.0 km in length beginning offshore of the second sand bar, allowing the AUV to be flown at an elevation of 3.0 m above the bottom for the entire mission and recorded both continuous, high resolution, side scan sonar imagery at 600 kHz and downward looking high definition (HD), geo-rectified, color photographs at 1 s intervals. The AUV traveled at a survey speed of 2.5 kts (1.3 m/s) and acquired a photograph every 1.3 m. The survey mission pattern is provided in Fig. 16.

The resulting Side Scan Sonar (SSS) images are present in Fig. 17. Upon close inspection of all eleven of these SSS images, distinct sedimentation patterns are observed. The northern most three survey lines are extremely uniform in texture and show a uniform bottom covered by sand extending from nearshore to the end of the survey line in approximately 11.0 m (36.1 feet) of water at the time of the survey (10 m depth chart datum IGLD85). As expected, the northern fillet is a sand-rich environment out to and beyond the characteristic depth of closure for Lake Michigan. The numerical simulation also showed that the offshore area beyond the second bar is dominated by sediment deposition (Fig. 13c1). In contrast, the three SSS survey lines adjacent to the harbor structures show a distinct sharp change in bottom texture at approximately 10 m water depth (33.3 feet) from fully sand covered shoreward, to sand starved offshore of that transition point (Fig. 17b). This delineation is clearly shown in Fig. 17c, an enlargement of the transition zone in the survey line directly north of the north harbor jetty. This is also represented in the numerical simulation, which showed sediment deposited at the region between 100 to 400 m of the mouth of the jetty and the deposition decreased sharply beyond 400 m (Fig. 13c1). To the south of the south harbor jetty, the degree of sand starvation increases from similarly fully sand covered out to approximately 10 m depth near the structure to almost non-existent to the far south of the study area. The most southerly three SSS survey lines show sediment only exists in

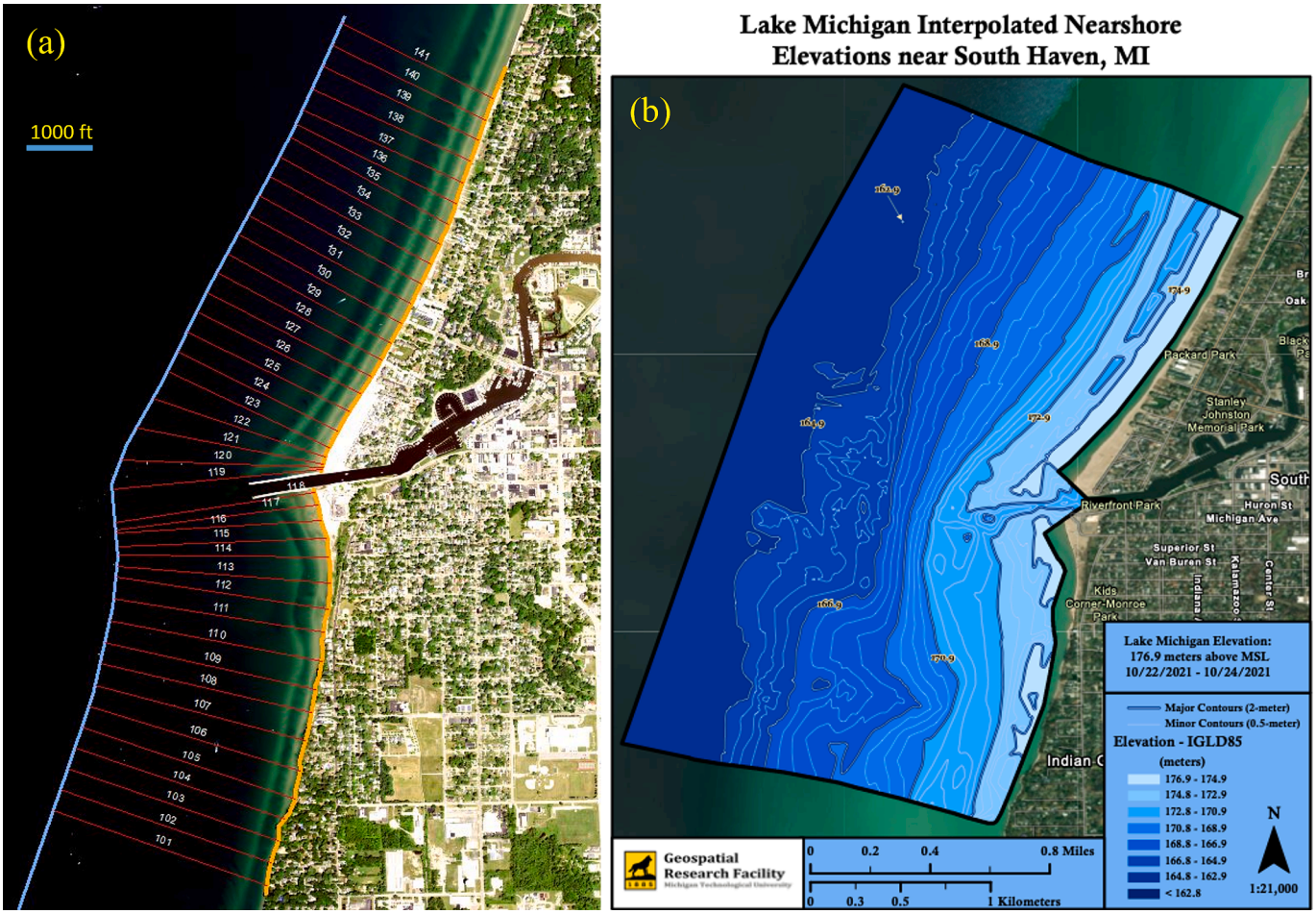

Fig. 15. (a) Survey profiles placed at 100-m intervals, perpendicular to the shoreline and extending approximately 2.0 km to the north of the north harbor jetty and 1.9 km south of the south harbor jetty at South Haven. (b) Rectified bathymetry around South Haven jetty in October 2021.

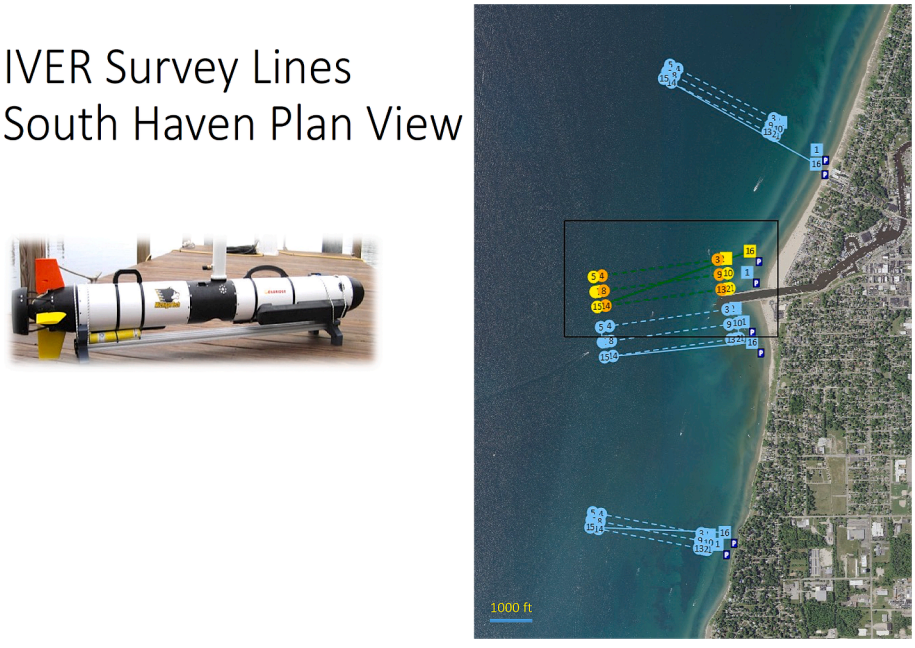

Fig. 16. Survey mission conducted with IVER 3 AUV.

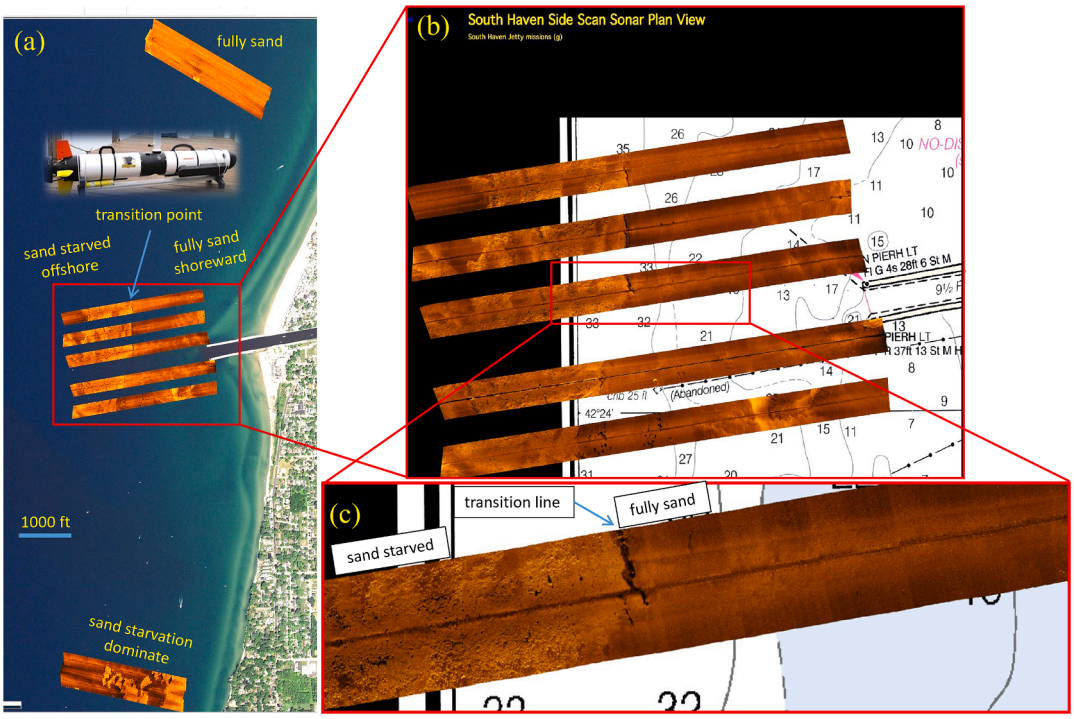

Fig. 17. (a) Images of all 11 survey lines collected by the IVER3 AUV, geospatially rectified to their GPS positions. (b) Enlargement of the five Side Scan Sonar (SSS) survey lines (three lines to the north and two lines to the south) of the end of the South Haven harbor jetties. (c) Enlargement of the SSS survey line directly to the north of the north harbor jetty. The high-resolution versions of the SSS processed images of each survey line are available online in the Electronic Supplementary Materials, Figs. S1-S3.

the very nearshore, terminating at a bottom elevation 171.9 m or a depth of 4.1 m or 13.4 feet (IGLD85). This is consistent with the numerical simulation, which shows that the far south of the southern jetty is dominated by sediment erosion (Fig. 13c1).

As further verification of the presence or absence of nearshore sediment existing on the lakebed, Fig. 18 is an enlarged section of the entire SSS survey line north of the north harbor jetty with the HD bottom photographs superimposed at their recorded GPS position along the transect. Unfortunately, at the time of the post storm survey, suspended fine sediment was still present in the water column. Although the water clarity in the color photographs is not good, there are distinct changes in bottom texture observed. The photographs shoreward of the transition line (Fig. 18d-e) show the presence of a sand bottom, consistent with the side scan sonar imagery from the same location. Offshore of the

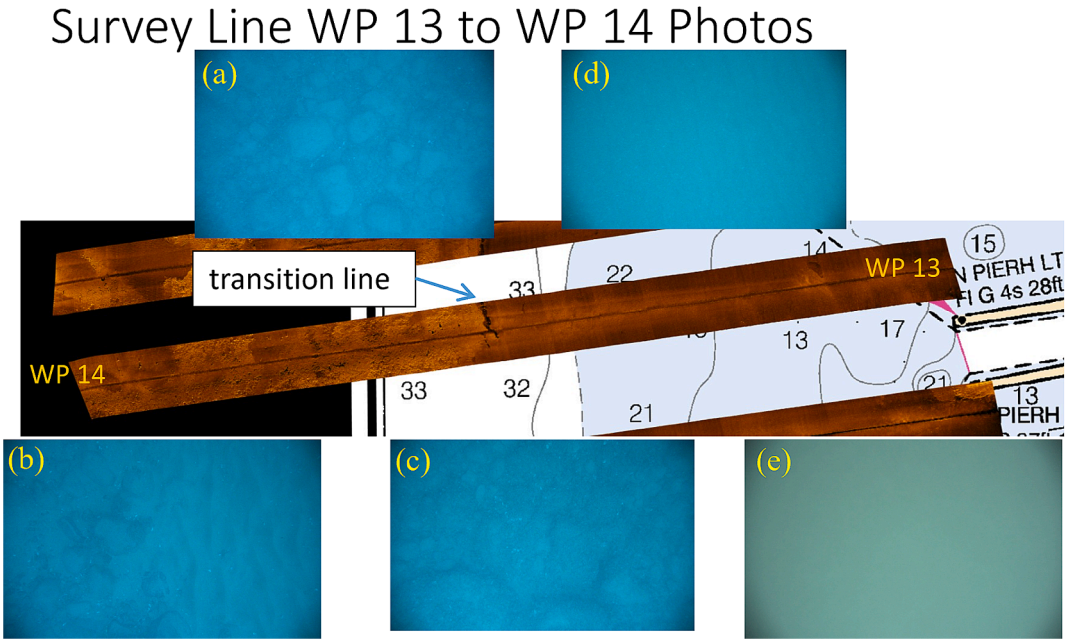

Fig. 18. Enlarged section of the entire Side Scan Sonar (SSS) survey line north of the north harbor jetty with the HD bottom photographs superimposed at their recorded GPS position along the transect. Photos (a) to (c) were taken on the offshore side of the transition line, while photos (d) and (e) were taken on the shoreward side.

transition line, the bottom becomes dominated by patches of the absence of sand and possibly exposed clay or cobblestone features (Fig. 18a-c). The presence of sand depleted regions increases moving south of the south jetty. Although qualitative, these observations provide some level of validation of the presence and absence of sand supply.

4. Conclusions

In this study, we simulate sediment transport and the sediment budget around a pair of mid-sized harbor jetties at South Haven, MI, in southern Lake Michigan using a coupled wave-current-sediment model. During selected individual storm events, longshore sediment transport decreases upstream of the jetties compared to scenarios without them, with an even greater reduction downstream. Throughout the navigation season (April to December), storm-driven currents predominantly cause southward longshore sediment transport. The jetties induce a large eddy downstream of the south jetty, generating a circulation that redirects the nearshore sediment transport northward adjacent to the south jetty. Over the entire navigation period, longshore sediment transport increases updrift of the jetties but decreases significantly downdrift. This results in sediment accretion on both sides of the jetty complex, forming a fillet pattern that expands the beaches at these locations. However, the area further south of the jetties experiences severe erosion. Understanding the dynamics of sediment transport and budget, particularly influenced by the jetties, is essential for resilient coastal management, ensuring beach safety and optimizing sites for dredging and nourishment. Future research will focus on assessing the impact of the jetties on shoreline changes, especially in light of fluctuating water levels.

CRediT authorship contribution statement

Longhuan Zhu: Writing – review & editing, Writing – original draft, Visualization, Validation, Software, Methodology, Investigation, Formal analysis, Data curation. **Guy A. Meadows:** Writing – review & editing, Writing – original draft, Visualization, Resources, Methodology, Formal analysis. **Miraj B. Kayastha:** Software, Methodology. **Pengfei Xue:** Writing – review & editing, Writing – original draft, Visualization, Validation, Supervision, Software, Resources, Project administration, Methodology, Investigation, Funding acquisition, Formal analysis, Data curation, Conceptualization.

Declaration of Competing Interest

The authors declare that they have no known competing financial interests or personal relationships that could have appeared to influence the work reported in this paper.

Acknowledgments

This is contribution no. 127 of the Great Lakes Research Center at Michigan Technological University. The Michigan Tech high performance computing cluster, *Superior*, was used in obtaining the modeling results presented in this publication. This work is sponsored by the Michigan Sea Grant College Program, Project Number Index R/SD-5, under award NA18OAR4170102 from National Sea Grant, NOAA, U.S. Department of Commerce, with funds from the State of Michigan. This project is also partly supported by the U.S. Department of Energy, Office of Science, under award number DE-SC0024446, as part of the Center for Climate-driven Hazard Adaptation, Resilience, and Mitigation (C-CHARM). Hydrodynamic modeling is also supported by COMPASS-GLM, a multi-institutional project supported by the U.S. Department of Energy, Office of Biological and Environmental Research, Earth and Environmental Systems Modeling program. Hydrodynamic modeling is also supported by the Great Lakes Restoration Initiative, through the University of Michigan Cooperative Institute for Great Lakes Research (CIGLR) cooperative agreement under the grant NA17OAR4320152. Hydrodynamic modeling is also supported by the National Aeronautics and Space Administration, Grant 80NSSC17K0287. The hydrodynamic work is also supported by Cooperative Agreement No. G21AC10141 from the United States Geological Survey. The statements, findings, conclusions, and recommendations of the authors expressed herein do not necessarily state or reflect those of the United States Government or any agency thereof. Finally, the authors would like to thank the anonymous reviewers for constructive comments that helped to improve this manuscript greatly.

Appendix A. Supplementary data

Supplementary data to this article can be found online at https://doi.org/10.1016/j.jglr.2024.102499.

References

Barnes, P.W., Kempema, E.W., Reimnitz, E., McCormick, M., 1994. The Influence of Ice on Southern Lake Michigan Coastal Erosion. *J. Great Lakes Res.* 20 (1), 179–195. https://doi.org/10.1016/S0380-1330(94)71139-4.

Beletsky, D., Schwab, D., 2008. Climatological circulation in Lake Michigan. Geophysical Research Letters 35 (21), 1–5. https://doi.org/10.1029/2008GL035773.

Booij, N., Ris, R.C., Holthuijsen, L.H., 1999. A third-generation wave model for coastal regions 1. Model description and validation. *J. Geophys. Res. Oceans* 104 (C4), 7649–7666. https://doi.org/10.1029/98JC02622.

Cardenas, M.P., Schwab, D.J., Eadie, B.J., Hawley, N., Lesht, B.M., 2005. Sediment Transport Model Validation in Lake Michigan. *J. Great Lakes Res.* 31 (4), 373–385. https://doi.org/10.1016/S0380-1330(05)70269-0.

Chen, C., Liu, H., Beardsley, R.C., 2003. An unstructured grid, finite-volume, three-dimensional, primitive equations ocean model: Application to coastal ocean and estuaries. *J. Atmos. Oceanic Tech.* 20 (1), 159–186. https://doi.org/10.1175/1520-0426(2003)020<0159:AUGFVT>2.0.CO;2.

Dilley, R.S., Rasid, H., 1990. Human response to coastal erosion: Thunder Bay, Lake Superior. *J. Coast. Res.* 6 (4), 779–788.

Eadie, B., Lozano, S., 1999. Grain size distribution of the surface sediments collected during the Lake Michigan mass balance and environmental mapping and assessment programs. In *NOAA Technical Memorandum ERL GLERL*. ftp://anonymous:%22www.glerl%40noaa.gov%22@ftp.glerl.noaa.gov/publications/tech_reports/glerl-111/tm-111.pdf.

Flor-Blanco, G., Pando, L., Morales, J.A., Flor, G., 2015. Evolution of beach–dune fields systems following the construction of jetties in estuarine mouths (Cantabrian coast, NW Spain). *Environ. Earth Sci.* 73 (3), 1317–1330. https://doi.org/10.1007/s12665-014-3485-1.

Garel, E., Sousa, C., & Ferreira. (2015). Sand bypass and updrift beach evolution after jetty construction at an ebb-tidal delta. *Estuarine, Coastal and Shelf Science, 167*, 4–13. doi: 10.1016/j.ecss.2015.05.044.

Hawley, N., Harris, C.K., Lesht, B.M., Clites, A.H., 2009. Sensitivity of a sediment transport model for Lake Michigan. *J. Great Lakes Res.* 35 (4), 560–576. https://doi.org/10.1016/j.jglr.2009.06.004.

Huang, C., Zhu, L., Ma, G., Meadows, G.A., Xue, P., 2021. Wave Climate Associated With Changing Water Level and Ice Cover in Lake Michigan. *Front. Mar. Sci.* 8 (November), 1–18. https://doi.org/10.3389/fmars.2021.746916.

Khazaei, B., Bravo, H.R., Anderson, E.J., Klump, J.V., 2021. Development of a Physically Based Sediment Transport Model for Green Bay, Lake Michigan. *J. Geophys. Res. Oceans*. https://doi.org/10.1029/2021jc017518.

Leatherman, S.P., Zhang, K., Douglas, B.C., 2000. Sea level rise shown to drive coastal erosion. *Eos* 81 (6), 55–57. https://doi.org/10.1029/00EO00034.

Lee, C., Schwab, D.J., Hawley, N., 2005. Sensitivity analysis of sediment resuspension parameters in coastal area of southern Lake Michigan. *J. Geophys. Res. Oceans* 110 (C3), 1–16. https://doi.org/10.1029/2004JC002326.

Lin, Y.T., Wu, C.H., 2014. A field study of nearshore environmental changes in response to newly-built coastal structures in Lake Michigan. *J. Great Lakes Res.* 40 (1), 102–114. https://doi.org/10.1016/j.jglr.2013.12.013.

Lou, J., Schwab, D.J., Beletsky, D., Hawley, N., 2000. A model of sediment resuspension and transport dynamics in southern Lake Michigan. *J. Geophys. Res. Oceans* 105 (C3), 6591–6610. https://doi.org/10.1029/1999JC900325.

Meadows, G.A., Meadows, L.A., Wood, W.L., Hubertz, J.M., Perlin, M., 1997. The Relationship between Great Lakes Water Levels, Wave Energies, and Shoreline Damage. *Bull. Am. Meteorol. Soc.* 78 (4), 675–682. https://doi.org/10.1175/1520-0477(1997)078<0675:TRBGLW>2.0.CO;2.

Mellor, G.L., Yamada, T., 1982. Development of a Turbulence Closure Model for Geophysical Fluid Problems. *REVIEWS OF GEOPHYSICS AND SPACE PHYSICS* 20 (4), 851–875. https://doi.org/10.1029/RG020i004p00851.

Paprotny, D., Terefenko, P., Giza, A., Czapliński, P., Vousdoukas, M.I., 2021. Future losses of ecosystem services due to coastal erosion in Europe. *Sci. Total Environ.* 760. https://doi.org/10.1016/j.scitotenv.2020.144310.

Roebeling, P.C., Costa, L., Magalhães-Filho, L., Tekken, V., 2013. Ecosystem service value losses from coastal erosion in Europe: Historical trends and future projections. *J. Coast. Conserv.* 17 (3), 389–395. https://doi.org/10.1007/s11852-013-0235-6.

Saengsupavanich, C. (2019). Willingness to restore jetty-created erosion at a famous tourism beach. *Ocean and Coastal Management*, *178*(April), 104817. doi: 10.1016/j.ocecoaman.2019.104817.

Smagorinsky, J., 1963. General circulation experiments with the primitive equations: I. The Basic Experiment. *Monthly Weather Review* 91 (3), 99–164. https://doi.org/10.1175/1520-0493(1963)091<0099:GCEWTP>2.3.CO;2.

Soulsby, R., 1997. *Dynamics of Marine Sands: A Manual for Practical Applications*. Thomas Telford Publications.

Theuerkauf, E.J., Braun, K.N., 2021. Rapid water level rise drives unprecedented coastal habitat loss along the Great Lakes of North America. *J. Great Lakes Res.* 47 (4), 945–954. https://doi.org/10.1016/j.jglr.2021.05.004.

Theuerkauf, E.J., Braun, K.N., Nelson, D.M., Kaplan, M., Vivirito, S., Williams, J.D., 2019. Coastal geomorphic response to seasonal water-level rise in the Laurentian Great Lakes: An example from Illinois Beach State Park, USA. *J. Great Lakes Res.* 45 (6), 1055–1068. https://doi.org/10.1016/j.jglr.2019.09.012.

Thiruvenkatasamy, K., & Baby Girija, D. K. (2014). Shoreline evolution due to construction of rubble mound jetties at Munambam inlet in Ernakulam-Trichur district of the state of Kerala in the Indian peninsula. *Ocean and Coastal Management*, *102*(PA), 234–247. doi: 10.1016/j.ocecoaman.2014.09.026.

Troy, C.D., Cheng, Y.T., Lin, Y.C., Habib, A., 2021. Rapid lake Michigan shoreline changes revealed by UAV LiDAR surveys. *Coast. Eng.* 170 (September), 104008. https://doi.org/10.1016/j.coastaleng.2021.104008.

Van Rijn, L. C. (2011). Coastal erosion and control. *Ocean and Coastal Management*, *54* (12), 867–887. doi: 10.1016/j.ocecoaman.2011.05.004.

Volpano, C.A.A., Zoet, L.K.K., Rawling, J.E.E., Theuerkauf, E.J.J., Krueger, R., 2020. Three-dimensional bluff evolution in response to seasonal fluctuations in Great Lakes water levels. *J. Great Lakes Res.* 46 (6), 1533–1543. https://doi.org/10.1016/j.jglr.2020.08.017.

Wang, Y.H., Wang, Y.H., Deng, A.J., Feng, H.C., Wang, D.W., Guo, C.S., 2022. Emerging Downdrift Erosion by Twin Long-Range Jetties on an Open Mesotidal Muddy Coast, China. *Journal of Marine Science and Engineering* 10 (5), 1–16. https://doi.org/10.3390/jmse10050570.

Warner, J.C., Sherwood, C.R., Signell, R.P., Harris, C.K., Arango, H.G., 2008. Development of a three-dimensional, regional, coupled wave, current, and sediment-transport model. *Comput. Geosci.* 34 (10), 1284–1306. https://doi.org/10.1016/j.cageo.2008.02.012.

Williams, A. T., Rangel-Buitrago, N., Pranzini, E., & Anfuso, G. (2018). The management of coastal erosion. *Ocean and Coastal Management*, *156*, 4–20. doi: 10.1016/j.ocecoaman.2017.03.022.

Xue, P., Pal, J.S., Ye, X., Lenters, J.D., Huang, C., Chu, P.Y., 2017. Improving the simulation of large lakes in regional climate modeling: Two-way lake-atmosphere coupling with a 3D hydrodynamic model of the great lakes. Journal of Climate 30 (5), 1605–1627. https://doi.org/10.1175/JCLI-D-16-0225.1.

Zhu, L., Xue, P., Meadows, G.A., Huang, C., Ge, J., Troy, C.D., Wu, C.H., 2024. Trends of sediment resuspension and budget in southern Lake Michigan under changing wave climate and hydrodynamic environment. *J. Geophys. Res. Oceans* 129 (4). https://agupubs.onlinelibrary.wiley.com/doi/pdf/10.1029/2023JC020180.